

Effect of shockwave-induced density jump on laser plasma interactions in low-pressure ambient air

Y Tao, M S Tillack, S S Harilal, K L Sequoia, B O'Shay and F Najmabadi

Department of Mechanical and Aerospace Engineering and the Center for Energy Research, University of California San Diego, 9500 Gilman Drive, La Jolla, CA 92093-0438, USA

Received 20 May 2006, in final form 18 July 2006

Published 1 September 2006

Online at stacks.iop.org/JPhysD/39/4027

Abstract

The dynamics of laser-produced plasma (LPP) and its shockwave-induced density jump (SIDJ) were investigated in low-pressure ambient air during the laser pulse using an optical interferometer. A tiny SIDJ could be observed clearly in ambient air with pressure as low as 3 Torr even during the rising edge of a 7 ns laser pulse. It was shown that the density jump and ionization could seed laser-induced ambient air breakdown at a relatively low pressure, which could significantly reduce laser energy deposited in the LPP. The ionization of the density jump was confirmed by dynamic emission imaging.

(Some figures in this article are in colour only in the electronic version)

Laser-produced plasma (LPP) in ambient gas has been investigated widely for a long time, motivated by applications of pulsed laser deposition (PLD), spectroscopic analysis, etc [1]. In recent times, interest has grown in the use of ambient gas with pressures from 10^{-2} to 100 Torr to mitigate debris from plasma in several LLP applications, such as a soft x-ray source for microscopy [2], an extreme ultraviolet lithography (EUVL) source [3] and laser fusion [4]. During the interaction of an intense laser pulse with a solid target in low-pressure ambient gas, plasma is generated first in the surface of the solid target. The resulting plasma expansion produces a compression wave in the solid material and a strong shockwave in the ambient gas. LPP and its compression wave into solid density material have been studied widely in the fields related to laser fusion [5]. Most of the previous work on LPP and its shockwave in ambient gas have been motivated by research relevant to PLD and mainly focus on the propagation of plasma plume in the ambient gas [6]. Some efforts to characterize LPP and its shockwave showed interesting results only at late time (after laser pulse) [7] and at high pressures [8].

Most of the physical processes of laser plasma interaction, including ionization, energy absorption, radiation transport etc occur during the laser pulse. However shockwaves and other processes, like three-body recombination, charge exchange and radiation heating occurring during the interaction of expanding plasma with ambient gas [9], could significantly

modify the interaction of the laser with solid plasma. So it is highly desirable to characterize LPP and its shockwave in ambient gas during the laser pulse to understand the effect of shockwaves on laser plasma interactions.

In this report, the dynamics of LPP and its shockwave-induced density jump (SIDJ) during the laser pulse in background air were investigated using an optical interferometer with high spatial and temporal resolution. The high sensitivity of the interferometer makes it possible to observe the propagation of shockwaves in ambient gas with low pressure at early time. Our efforts focus on the influence of the shockwave on the laser plasma interactions.

Experiments were carried out using a Nd:YAG laser (Continuum Surelite II 10), which can produce a laser pulse at $1.064 \mu\text{m}$ with energy of 650 mJ at 10 Hz. The beam diameter is 7 mm. The temporal pulse shape of the laser is close to a Gaussian with a width (FWHM) of 7 ns. The base width, defined by the times when the intensity exceeds 10% of the peak value, is 15 ns. A small part split from the main laser beam is converted into green light (532 nm) by a type II KDP crystal and used as a probe beam. The main laser beam is focused with a lens with a focal length of 100 mm onto the surface of a 2 mm thick Al plate at normal incidence in a vacuum chamber, which can be pumped down to 10^{-6} Torr. The focus of the laser beam was placed behind the target surface to obtain a diameter (FWHM) of $130 \mu\text{m}$. The target is moved to maintain a fresh surface for each shot.

A Nomarski interferometer [10] was employed to observe the density profile of LPP and its SIDJ. A convex F/15 lens relays the plasma image to an imager, with the Nomarski interferometer inserted in front of the imager. The interferometer consists of a Wollaston prism and a cube polarizer. The interferogram is recorded with an intensified charge coupled device (ICCD) camera (Princeton, PI-MAX). The fastest gated interval of 2 ns is always used in our experiments. The gate is triggered by a signal from the laser controller, with jitter less than 0.5 ns. The spatial resolution of the interferometer was calibrated by taking a shadowgraph of a 150 μm Cu wire. In these experiments it was less than 25 μm with a 7 \times magnification. A narrow band interference filter is employed to block the broadband plasma emission. Shadowgraphs of LPP and its SIDJ were observed using the same experimental arrangement with that used in the interferometer, except that the cube polarizer was rotated to block one of the beams split by the Wollaston prism. Dynamic emission imaging was performed with the same imaging lens and ICCD camera used in the interferometer, with the probe laser blocked and the magnification kept the same as the interferometer.

A typical interferogram of LPP and its shockwave in ambient atmosphere at the peak of laser pulse is shown in figure 1(a). In this case, the pressure is 7 Torr. The laser enters from the right hand in the image. The peak laser intensity is always $2 \times 10^{11} \text{ W cm}^{-2}$ for all of the following experiments. The initial target surface is marked by the white line shown in figure 1(a). There are two regions containing obvious fringe shifts: one is located close to the target surface in the centre of the image and the other is an outer fringe shift accompanied by a semi-annular dark ring. The central part is induced by LPP. Its expansion into ambient atmosphere is obvious; the dark region near the target surface arises from the opacity of the plasma with density above the critical density ($3.9 \times 10^{21} \text{ W cm}^{-2}$ for wavelength of 532 nm). The outer fringe shift comes from the density jump induced by a shockwave arising from the expansion of LPP. The expansion of LPP sweeps up the ambient atmosphere and results a pile-up of atoms. A 2D phase shift map was extracted from the interferogram shown in figure 1(a) with a mathematical treatment based on the fast Fourier transform (FFT) [11] and a 2D density map was deduced from the phase shift map employing an Abel inversion [12]. The 2D density map is shown in figure 1(b). The SIDJ is clearly seen in figure 1(b). It shows a semi-elliptical shape centred at the LPP. Its amplitude increases with the decrease in the angle with respect to the normal direction, and the peak appears in the normal direction. This coincides with the known 2D expansions of LPP when a finite focal spot is employed [11]. The rarefied region with a lower density between LPP and SIDJ is also noted in figure 1(b).

For the highly ionized LPP, the fringe shift comes mainly from the electrons. However, for partially ionized SIDJ, the fringe shift is induced by both electrons and neutral atoms. The electron density shown in figure 1(b) should be corrected by taking account of the fringe shift induced by neutral atoms. The refractive index of the mixture of electron and neutral atoms can be described as [13]

$$n = 1 - \frac{n_e}{2n_c} + \beta \frac{\rho}{\rho_0}, \quad (1)$$

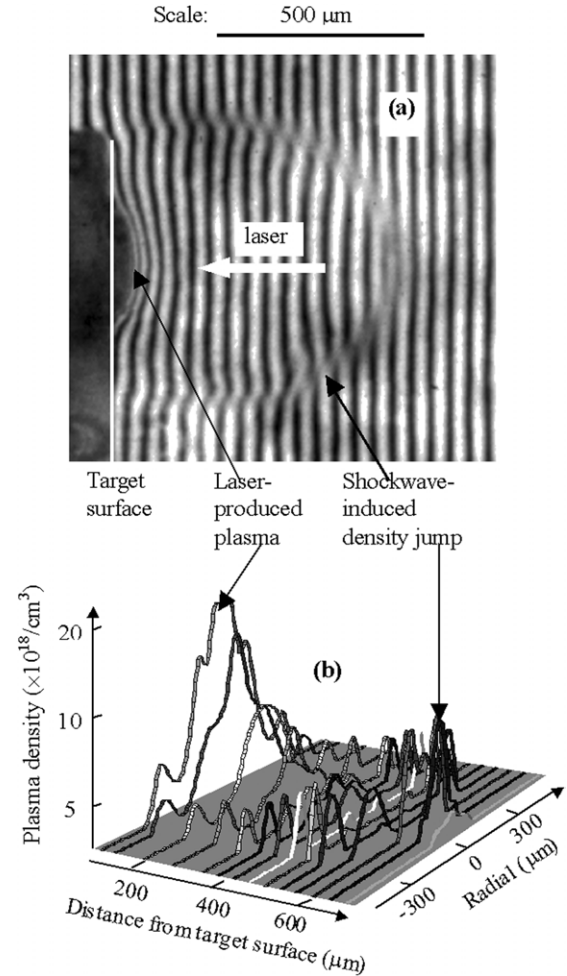


Figure 1. (a) Typical interferogram and (b) 2D density profile of LPP and its SIDJ in ambient air with a pressure of 7 Torr.

where $n_c = 1.1 \times 10^{21}/\lambda^2 \text{ cm}^{-3}$ is the critical density of the probe beam with the wavelength in units of μm ; $\beta = 2.9 \times 10^{-4}$, $\rho/\rho_0 = 2(M^2 - 1)/[(\gamma - 1)M^2 + 2]$ is the compressed ratio of the densities of neutral atoms in front of and behind the shockwave front, $M = v/c_s$ is the Mach number of the shockwave, v and c_s are the velocities of the shockwave front and sound, respectively and $\gamma = 1.4$ is the heat capacity ratio of air. It is seen that the fringe shifts induced by electrons and neutral atoms are obtained in opposite directions. In figure 1(a), the fringe shift induced by electrons is towards the right, and neutral atoms contribute to a fringe shift towards the left. It is seen in figure 1(a) that the fringes are mainly shifted towards the right. This shows that electrons are dominant even inside the SIDJ. The corrected electron density inside the SIDJ can be described as $n_e = 2n_c(\frac{n'_e}{2n_c} + \beta \frac{\rho}{\rho_0})$, where n'_e is the plasma density inside the SIDJ as shown in figure 1(b). When the neutral atom effect is included, a higher electron density should be expected. From the interferograms observed at various times, the velocity of the shockwave at the peak of the laser pulse was deduced as $5 \times 10^6 \text{ cm s}^{-1}$, so $M = 150$, and then $\rho/\rho_0 = 5$. For a 0.532 μm probe light, $n_c = 3.9 \times 10^{21} \text{ cm}^{-3}$. Inside the SIDJ, the corrected electron density is $n_e = n'_e + 1.2 \times 10^{19} \text{ cm}^{-3}$. The electron

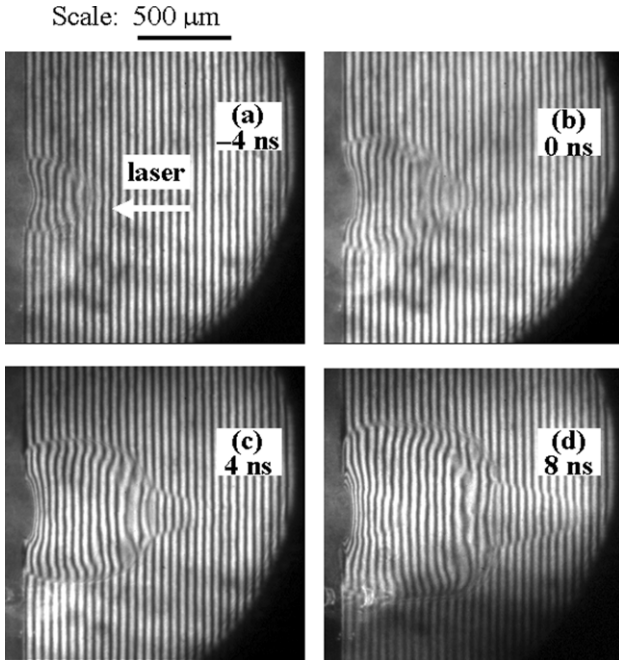


Figure 2. Interferograms of LPP and its SIDJ in ambient air with a pressure of 20 Torr at various times (a) -4, (b) 0, (c) 4 and (d) 8 ns.

density located in front of the shockwave front in the line of laser incidence should be $2 \times 10^{19} \text{ cm}^{-3}$.

In order to clarify the influence of SIDJ on laser plasma interactions, dynamic interferograms of LPP and its SIDJ in ambient air with various pressures from 0.1 to 100 Torr were observed during the laser pulse. It was noted that when the pressure is less than 20 Torr, SIDJ shows a perfect semi-elliptical form like that shown in figure 1(a). The results obtained at 20 Torr at various delay times of -4, 0, 4 and 8 ns, are shown in figures 2(a), (b), (c), and (d), respectively. The zero time represents the peak of the laser pulse. It is seen in figure 2(a) that in the initial stage (-4 ns) the shockwave front is still similar to those observed at lower pressures; however, at the peak of the laser pulse (0 ns) a distortion of the fringes appears on the top of the density jump, as shown in figure 2(b). This fringe distortion becomes more obvious at later times as shown in figures 2(c) and (d), and a cone-shaped plasma channel toward the focus lens appears at a later time as shown in figure 2(d). The cone-shaped plasma channel is known as the laser-induced breakdown of ambient air [13]. It is noted that the start of the breakdown is located at the front of the density jump and in the line of laser incidence.

The laser intensity in our experiments is much lower than the breakdown threshold of ambient atmosphere at 20 Torr, which is above $10^{12} \text{ W cm}^{-2}$ [14], and no breakdown was observed in the present experimental conditions when the solid target was removed. It is obvious that the breakdown is initialized by the SIDJ. The rising slope of the laser pulse produces LPP and its shockwave as shown as figure 2(a). The main part of the laser pulse intercepts the SIDJ in the line of laser incidence. There may be two possibilities to enhance the absorption of laser energy at the density jump: one is the local pressure enhancement [13], and the other may arise from ionization inside the density jump. The breakdown

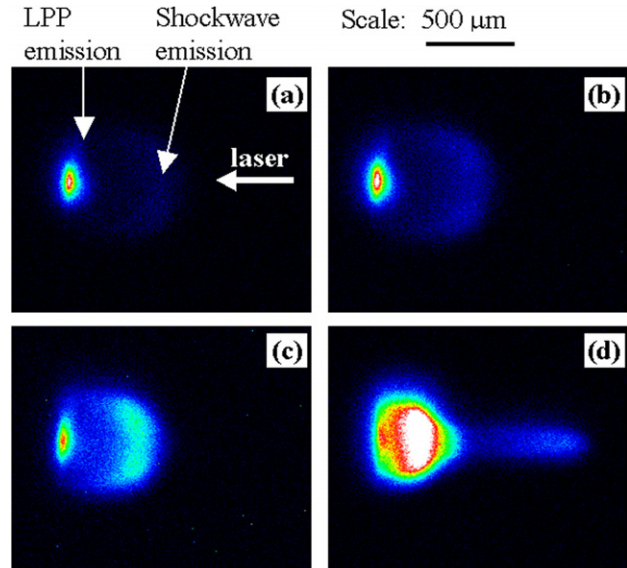


Figure 3. Emission images of LPP and SIDJ in ambient air with pressures of (a) 7, (b) 10, (c) 20 and (d) 100 Torr taken at the peak of the laser pulse.

threshold of ambient gas drops rapidly with an increase in pressure [14]. The dominant laser absorption mechanism in ambient atmosphere is an inverse Bremsstrahlung, which is proportional to the electron density of the plasma. The electrons inside the density jump could act as the initial seed electrons, and then most of the laser energy is absorbed via a cascade process, resulting in a breakdown of the ambient air. Laser-induced gas breakdown may strongly absorb laser energy [13]. Then the laser energy into the solid plasma is reduced, and the interaction of the laser with the solid target plasma will be modified significantly.

Dynamic emission imaging of LPP in ambient air with various pressures was performed under conditions identical with those used in the interferometer measurements. Images taken at pressures of 7, 10, 20 and 100 Torr at the peak of the laser pulse are shown in figures 3(a), (b), (c) and (d), respectively. It is seen that figure 3, in addition to the emission arising from LPP located at the centre of the images, there is a semi-elliptical emission region. The shape and size of the emission images shown in figures 3(a) and (c) coincide with those of the SIDJ shown in figure 1(a) and figure 2(b), respectively. We can conclude that the outer elliptical emission comes from the SIDJ. This may show that the atoms inside the density jump have been ionized significantly. Two possible mechanisms may contribute to the ionization. One is that electrons and short wavelength radiation from LPP ionize atoms in the ambient atmosphere, and then the shockwave piles up the ions to form a high density and bright emission region [3]. The other is that the ionization is induced by enhanced collisions inside the density jump. It is also noted in figure 3 that there is a weak emission region in the rarefied field behind the shockwave front. Because the electrons and radiation from the plasma are much faster than plasma expansion and shockwave, the emission intensity should be proportional to the density during the whole laser pulse. The atom density in the rarefied field should be less than that in the undistorted region located in front of the shockwave front, so that emission

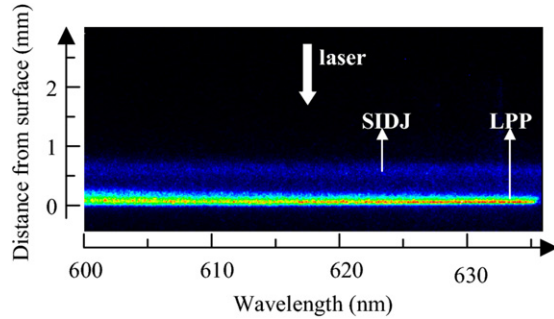


Figure 4. Spatially-resolved spectra of LPP and SIDJ taken at 7 Torr at 2 ns after the peak of the laser pulse.

from the undistorted region should be stronger than that in the rarefied field. However, emission from the undistorted region could not be observed at all. So in our case most of the ionization may arise from shockwave-enhanced collisions. The rarefied field emission may come from the remaining ions piled up by the previous shockwave front. With the increase in pressure, shock-induced emission becomes brighter, but LPP emission becomes weaker. Emission due to a laser-induced ambient atmosphere breakdown at high pressure is also seen in figure 3(d). It shows that significant laser energy is deposited in ambient gas rather than in solid plasma at high pressure. This confirms the conclusion mentioned above from interferometry measurements.

To confirm the ionization inside the SIDJ, a spatially-resolved spectral of the SIDJ was observed by a triple-grating spectrometer (Acton Spectra-Pro 500i) equipped with a time-gated ICCD camera. The emission image is rotated by a pair of orthogonal Al mirrors and the centre part along the line of laser incidence is relayed to the slit of the spectrometer. A typical spatially-resolved spectral from laser-produced Al plasma observed in a 7 Torr pressure air at a time 2 ns after the peak of the laser pulse is shown in figure 4. The gate time of the ICCD camera is 2 ns. It is seen that there are two separated emission regions; one near the target surface comes from the LPP, the other comes from the SIDJ. The shape and size of the two emission regions are consistent with those shown in figure 3(a). The emission from the SIDJ is in continuum. It was also found that in the wavelength range from 320 nm to 1 μm emission from the SIDJ is also nearly in continuum. The continuum comes from the electron transitions of free-free and free-bond. The strong lines from N^{2+} , for instance, 500.15 ($3p^3D_2 - 3d^3F_3^0$) and 500.5 ($3p^3D_3 - 3d^3F_4^0$) nm, were also observed at a late time (after 150 ns). This confirms that air inside the SIDJ is significantly ionized.

To check the sensitivity of the interferometer, interferograms and shadowgraphs were taken at various pressures from 0.1 to 100 Torr. The laser intensity is kept constant at $2 \times 10^{11} \text{ W cm}^{-2}$. Clear interferograms of the SIDJ could be achieved at -4 ns with respect to the peak of the laser pulse at a pressure as low as 3 Torr. For comparison, it is hard to obtain clear shockwave tracks in the shadowgraphs during the laser pulse at a pressure less than 20 Torr. This result confirms

the lower sensitivity of the shadowgraph to characterize shockwaves as mentioned by Gregory *et al* [8]. The reason comes from the fact that interferogram information arises from the fringe shift that does not strongly depend on the uniformity of the background, while shadowgraphy strictly requires a uniform background. However, in general, in order to achieve high temporal resolution, a pulsed laser is generally used as the probe beam. And the uniformity of commercially available high power pulsed lasers is limited. So an optical interferometer is more suitable for the investigation of LPP and its shockwave in ambient gas during the laser pulse.

In conclusion, the dynamics of LPP and its SIDJ in ambient atmosphere have been measured simultaneously with an optical interferometer. Compared with shadowgraphy, the higher sensitivity of interferometry makes it possible to measure the tiny SIDJ in ambient gas with a pressure as low as 3 Torr at early time. It is found that the SIDJ and ionization could modify the breakdown threshold of the ambient air, significantly reducing the laser energy into the solid plasma. In research related to applications of laser fusion and soft x-ray source etc, much higher shockwave velocity from much higher laser intensity and strong ionization of ambient gas induced by strong short-wavelength emission from high-Z plasmas will enhance the effect of the SIDJ even when lower pressure ambient gas is used, so further experimental and theoretical efforts should be carried out to clarify the effect of ambient gas under the specific conditions for those applications.

References

- [1] Hughes T P 1975 *Plasmas and Laser Light* (New York: Wiley)
- [2] Kuhne M and Petzold H-C 1984 *Opt. Lett.* **9** 16
- [3] Harilal S S, O'Shay B, Tao Y and Tillack M S 2006 *J. Appl. Phys.* **99** 083303
- [4] Stampera J A, Lehmborg R H, Leheckab T, Denizc A V, McLeana E A and Sethian J D 2004 *Nucl. Fusion* **44** 745-51
- [5] Eliezer S 2002 *The Interaction of High-Power Lasers and Plasmas* (Bristol: Institute of Physics Publishing)
- [6] Geohegan D B 1992 *Thin Solid Films* **220** 138
- [7] Amoroso S, Bruzzese R, Spinelli N and Velotta R 1999 *J. Phys. B: At. Mol. Opt. Phys.* **32** R131
- [8] Ni X-Wu, Lu J, Zhi A, Ma H-Z, and Zhou J-L 1989 *Opt. Comm.* **74** 185
- [9] Gregory C D, Courtois C, Hall I M, Howe J and Woolsey N C 2005 *Central Laser Facility Annual Report 2004/2005* p 70
- [10] Hauer M, Funk D J, Lippert T and Wokaun A 2004 *Thin Solid Films* **453** 584
- [11] Chowdhury A, Arora V, Naik P A and Gupta P D 2003 *J. Appl. Phys.* **93** 3218
- [12] Benattar R, Popovics C and Sigel R 1979 *Rev. Sci. Instrum.* **50** 1583
- [13] Tao Y, Nishimura H, Fujioka S, Sunahara A, Nakai M, Okuno T, Ueda N, Nishihara K, Miyanaga N and Izawa Y 2005 *Appl. Phys. Lett.* **86** 201501
- [14] <http://optics.tu-graz.ac.at/>
- [15] Zeldovich B Y and Raizer P Y 1966 *Physics of Shock Waves and High-Temperature Hydrodynamic Phenomena* (New York: Academic)
- [16] Ireland C L M 1974 *J. Phys. D: Appl. Phys.* **7** L179